Acta Pharmacologica Sinica (2015) 36: 1266–1276
 1671-4083/15
www.nature.com/aps

Original Article

DCLAK11, a multi-tyrosine kinase inhibitor, exhibits potent antitumor and antiangiogenic activity *in vitro*

Xiao-bin GUO[1, 3], Wei ZHU[2], Xian-jie CHEN[2], Lin-jiang TONG[3], Xia PENG[3], Min HUANG[3], Hong-chun LIU[3], Hong LIU[2], Jian DING[3, *]

[1]*Department of Clinical Pharmacology, Xiangya Hospital and Institute of Clinical Pharmacology, Central South University, Changsha 410078, China;* [2]*CAS Key Laboratory of Receptor Research;* [3]*Division of Anti-tumor Pharmacology, State Key Laboratory of Drug Research, Shanghai Institute of Materia Medica, Chinese Academy of Sciences, Shanghai 201203, China*

Aim: To investigate the molecular targets of DCLAK11, a novel compound discovered from a series of substituted pyridin-3-amine derivatives, and to characterize its anti-tumor properties *in vitro*.
Methods: Kinase inhibition was measured by an ELISA assay. Cell viability was assessed with an SRB or a CCK8 assay. The alterations induced by kinase signaling proteins in cancer cells were detected by Western blot. Apoptosis was determined by an Annexin V-PI assay. The following assays were used to evaluate the impact on angiogenesis: wound-healing, Transwell, tube formation and microvessel outgrowth from rat aortic rings.
Results: DCLAK11 was a multi-targeted kinase inhibitor that primarily inhibited the EGFR, HER2, and VEGFR2 tyrosine kinases with IC_{50} value of 6.5, 18, and 31 nmol/L, respectively. DCLAK11 potently inhibited the proliferation of EGFR- and HER2-driven cancer cells: its IC_{50} value was 12 and 22 nmol/L, respectively, in HCC827 and HCC4006 cells with EGFR exon deletions, and 19 and 81 nmol/L, respectively, in NCI-N87 and BT474 cells with HER2 amplification. Consistently, DCLAK11 blocked the EGFR and HER2 signaling in cancer cells with either an EGFR or a HER2 aberration. Furthermore, DCLAK11 effectively induced EGFR/HER2–driven cell apoptosis. Moreover, DCLAK11 exhibited anti-angiogenic activity, as shown by its inhibitory effect on the proliferation, migration and tube formation of human umbilical vascular endothelial cells and the microvessel outgrowth of rat aortic rings.
Conclusions: DCLAK11 is a multi-targeted kinase inhibitor with remarkable potency against tyrosine kinases EGFR, HER2 and VEGFR2, which confirms its potent anti-cancer activity in EGFR- and HER2-addicted cancers and its anti-angiogenic activity.

Keywords: DCLAK11; substituted pyridin-3-amine derivatives; tyrosine kinase; EGFR; HER2; VEGFR2; anticancer; anti-angiogenesis

Acta Pharmacologica Sinica (2015) 36: 1266–1276; doi: 10.1038/aps.2015.25; published online 18 May 2015

Introduction

Cancer is a complex, multi-factorial and devastating disease and the oncogenic behavior of tumor cells is driven by multiple signaling pathways. Dysfunctions in intracellular signaling pathways have also been implicated in the development and progression of cancer. Receptor tyrosine kinase (RTK) phosphorylation is now well recognized as a major regulatory mechanism of cell signaling and related activities[1]. Aberrant tyrosine phosphorylation is either the primary cause of human cancer or is required for maintenance of the oncogenic state[2, 3]. Abnormal RTK activation in cancer is often caused by gene amplification, receptor overexpression, autocrine activation, or gain-of-function mutations. For instance, epidermal growth factor receptor (EGFR) mutations in the kinase domain occur in 10%–40% of lung cancers[4], and among them, exon 19 deletion in EGFR accounts for 45%[5]. HER2 overexpression occurs in 20%–30% of breast cancers[6] and in approximately 22% of gastric cancers[7]. Mutations in the kinase domain of HER2 occur in 4% of all lung carcinomas and in 10% of lung adenocarcinomas[8].

Indeed, molecularly targeted therapies that inhibit RTK molecules that function in tumor growth or progression represent an important strategy for cancer therapy and have already led to important clinical results[9, 10]. Over 20 drugs that target tyrosine kinases have been approved by the US Food and Drug Administration[11]. However, acquisition of resistance within 1 or 2 years is common. After treatment with selective signal transduction inhibitors to block crucial pathways that are necessary for cell survival, drug-induced selective pressure and the genetic instability of cancer cells can activate multiple growth-control pathways in cancer cells and cause a switch to alternative survival mechanisms. This contributes to the

* To whom correspondence should be addressed.
E-mail jding@simm.ac.cn
Received 2015-03-10 Accepted 2015-04-03

development of acquired resistance to these drugs. Selective targeted agents seem to have limited single-agent activity, and therefore, a combination of molecular therapies that targets several pathways becomes a strong rational approach in the treatment of cancer.

EGFR is an RTK that belongs to the HER family of receptors[12]. The aberrant activity of EGFR, which promotes cell proliferation, angiogenesis, migration, survival, and adhesion, has been shown to play a key role in the development and growth of tumors[13]. EGFR is upregulated in a variety of tumors in a subset of patients with EGFR aberrations in which EGFR inhibitors have demonstrated clinical benefits[14]. Despite of their clinical success, resistance to EGFR inhibitors occurs frequently. One of the major mechanisms that leads to resistance of EGFR inhibitors is the activation of alternative survival pathways, which results from the upregulated RTKs. As such, the use of dual- or multiple-targeted kinase inhibitors has gained increased interest in the field. HER2 belongs to the same family as EGFR and is known as the favored dimerization partner for all of the other HER family members[15,16]. The HER2 heterodimer combinations with EGFR exhibit robust signaling activity[17]. Constitutive activation of HER2 results from HER2 gene amplification or from mutations that mediate multiple pathological responses including multi-drug resistance[18]. Concurrent targeting of EGFR and HER2 may lead to new therapeutic opportunities.

In addition to the effective inhibition of tumor cells by multi-kinase inhibitors, concurrent intervention with respect to the cancer microenvironment is an important approach that may strengthen the efficacy of anti-cancer drugs. The inhibition of angiogenesis, which plays an essential role in the survival of cancer cells, in terms of local tumor growth and in the development of distant metastasis[19, 20], provides an important anti-tumor strategy for solid tumors[21]. VEGF, as one of the most important angiogenic growth factors[22], initiates the recruitment and proliferation of nearby vessel structures and sustains the tumor neovasculature[23]. Members of the VEGFR family are important mediators of pro-angiogenic signals, and VEGFR signaling is imperative for tumor angiogenesis[24, 25]. In cancer cells, altered control of angiogenesis following enhanced VEGF expression may cause acquired resistance to EGFR inhibitors[26]. In contrast, EGFR/HER2 signaling activation can stimulate the synthesis and secretion of a number of angiogenic regulating factors such as VEGF[27]. A growing body of preclinical and clinical evidence suggests the use of either a combination of single EGFR and VEGFR inhibitors or agents with dual inhibition of both pathways, which were superior in terms of tumor growth inhibition than when these agents were given as a single treatment[28–31].

Inspired by the benefits of compounds that target multiple tyrosine kinases in cancer therapy, we screened a series of substituted pyridin-3-amine derivatives to explore the possibility of the concurrent targeting of EGFR and HER2. We were particularly interested whether a targeted spectrum of the compound would confer anti-angiogenic activity. This rationale led to the discovery of one derivative, DCLAK11 {(*R*)-4-chloro-2-[5-(2-hydroxy-1-phenylethylamino)-3-(3-methyl-1*H*-indazol-5-yl) pyridin-2-yl]phenol}. In this report, we identified DCLAK11 as a potent multi-targeted RTK inhibitor that concurrently targets EGFR, HER2, and VEGFR2, and assessed its anti-tumor activity. Our results suggested that DCLAK11 is a promising multi-targeted inhibitor that deserves further consideration.

Materials and methods

Synthesis of the compound DCLAK11

A series of substituted pyridin-3-amine derivatives was designed and synthesized at Prof Hong LIU's Laboratory in Shanghai Institute of Materia Medica. Compound DCLAK11(chemical structure shown in Figure 1, synthetic route shown in Supplementary Scheme 1) presented promising activities in a biological screening and was selected for further evaluation. The purity of DCLAK11 was 98%. In this study, DCLAK11 was dissolved to 10 mmol/L in DMSO as a stock solution and stored at -20 °C.

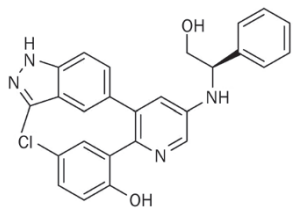

Figure 1. Chemical structures of DCLAK11.

Cell culture

Human umbilical vascular endothelial cells (HUVECs) were obtained from PromoCell (Heidelberg, Germany) and were used from passages 2 to 8 in our study. The immortalized human gastric epithelial mucosa cell line GES-1, the human hepatic cell line LO2, the hepatocellular carcinoma cell lines SMMC-7721 and BEL-7402, the human lung cancer cell line HCC827 and the human myeloid leukemia cell line HL-60 were all obtained from the Institute of Biochemistry and Cell Biology, Chinese Academy of Sciences (Shanghai, China). The following cell lines were obtained from the American Type Culture Collection (ATCC, Manassas, VA, USA): human gastric cancer cell lines NCI-N87 and SNU5, the human breast cancer cell lines MCF-7, MDA-MB-435, and BT474, the human squamous carcinoma cell line A-431, the human lung cancer cell lines HCC4006, H1975, and PC9, and the human prostate carcinoma cells DU145. The human gastric cancer cell lines MKN74, MKN45, and MKN1 were obtained from the Japanese Collection of Research Bioresources (Osaka, Japan). The cells were cultured as recommended at 37 °C with 5% CO_2 in a humidified incubator (Thermo Fisher Scientific, MA USA).

ELISA kinase assay

The effects of DCLAK11 on the activities of various tyrosine kinases were determined using enzyme-linked immunosor-

bent assay (ELISA), as described previously[32]. Briefly, 20 μg/mL of poly (Glu,Tyr)$_{4:1}$ substrate (Sigma, St Louis, MO, USA) was used to pre-coat 96-well plates. Then, 49 μL of 10 μmol/L ATP solution diluted in kinase reaction buffer [50 mmol/L HEPES (pH 7.4), 50 mmol/L $MgCl_2$, 0.5 mmol/L $MnCl_2$, 0.2 mmol/L Na_3VO_4, and 1 mmol/L DTT] was added to each well; 1 μL of various concentrations of DCLAK11 were diluted in DMSO (*v/v*) (Sigma, St Louis, MO, USA) and then added to each reaction well. The kinase reaction was initiated by the addition of purified tyrosine kinase proteins diluted in 50 μL of kinase reaction buffer and was performed in triplicate. After incubation for 60 min at 37 °C, the plate was washed three times with phosphate-buffered saline (PBS) containing 0.1% Tween 20 (T-PBS). Next, 100 μL anti-phosphotyrosine (PY99) antibody (1:500, diluted in T-PBS with 5 mg/mL BSA) (Santa Cruz Biotechnology, Santa Cruz, CA, USA) was then added; the plate was incubated at 37 °C for 30 min. After the plate was washed three times, 100 μL horseradish peroxidase-conjugated goat anti-mouse IgG (1:2000, diluted in 5 mg/mL BSA T-PBS, Calbiochem, San Diego, CA, USA) was added and the plate was incubated again at 37 °C for 30 min, then washed three times. A 100-μL aliquot of a solution of 0.03% H_2O_2 and 2 mg/mL *o*-phenylenediamine in citrate buffer (0.1 mol/L, pH 5.5) was added, and samples were incubated at room temperature until color emerged. The reaction was terminated by the addition of 50 μL of 2 mol/L H_2SO_4 as the color changed, and the absorbance at 490 nm was analyzed using a SpectraMax 190 Microplate Reader (Molecular Devices, Sunnyvale, CA, USA). The inhibition rate (%) was calculated with the following equation: [1–(A_{490}/A_{490} control)]×100. The inhibitory concentration (IC_{50}) values were calculated from the inhibition curves in three separate experiments.

Cell proliferation assay

Cells were seeded in 96-well culture plates (Corning Life Science, Tewksbury, MA, USA) at a density of 3000–8000 cells/well. On the following day, the cells were exposed to various concentrations of compounds and were cultured for another 72 h. Cell proliferation was then determined by sulforhodamine B (SRB) (Sigma-Aldrich, St Louis, MO, USA) or with the Cell Counting Kit-8 (CCK8) (Dojindo, Shanghai, China) assay. The absorbance was determined at 515 nm or 450 nm with a SpectraMax 190 Microplate Reader (Molecular Devices, USA). The inhibition rate (%) was calculated with the following equation: [($OD^{control}$–$OD^{treatment}$)/$OD^{control}$]×100. The IC_{50} values were calculated by a concentration response curve fitting using the four-parameter method.

VEGF-driven HUVEC proliferation assay

A total of 1×10^4 HUVECs was seeded in 96-well culture plate. The next day, the cells were serum-starved in medium with 1% FBS for 24 h. HUVECs were then exposed to various concentrations of compounds for 30 min followed by the addition of 50 ng/mL of VEGF165 (PeproTech, Rocky Hill, NJ, USA). HUVECs were cultured for another 72 h. Appropriate controls were included [cultured with 50 ng/mL VEGF165 (VEGF+) or not (VEGF–)]. Cell proliferation was determined by CCK8 assay according to the manufacturer's instructions. The absorbance at 450 nm was determined with a SpectraMax 190 Microplate Reader (Molecular Devices, USA). The VEGF-dependent proliferation inhibition %=[1–($OD^{treatment}$–OD^{VEGF-}/OD^{VEGF+}–OD^{VEGF-})]×100. The IC_{50} values were calculated by concentration response curve fitting using the four-parameter method.

Apoptosis assay

Cell apoptosis induced by DCLAK11 was detected with an Annexin V-FITC/PI Apoptosis Detection Kit (Vazyme Biotech, Piscataway, NJ, USA) in accordance with the manufacturer's protocols. Briefly, 1×10^5 NCI-N87, BT474, HCC827, and HCC4006 cells were collected and washed with PBS. The harvested cells were resuspended in binding buffer, followed by incubation with 5 μL of Annexin V-FITC and 5 μL of propidium iodide (PI) and were incubated for 10 min in the dark at room temperature. Apoptosis was analyzed with a FACS Calibur flow cytometer (BD Bioscience, San Jose, CA, USA), and the data were analyzed with FlowJo software (Tree Star, Inc Ashland, USA).

Western blot analysis

HCC827, HCC4006, NCI-N87, and BT474 cells were grown to 80%–90% confluence, exposed to the tested compounds for the indicated hours at 37 °C; HUVECs were serum-starved for 24 h, and then treated with the indicated dose of DCLAK11 for 6 h at 37 °C followed by stimulation with 50 ng/mL VEGF165 during the last 10 min. The cells were then lysed in 1×SDS sample buffer and subsequently resolved by SDS-PAGE and transferred to nitrocellulose membranes. The membranes were first probed with the indicated antibodies as follows: [phospho-VEGFR2 (Tyr 1175), VEGFR2, phospho-HER2 (Tyr1221/1222), phospho-EGFR (Tyr1068), EGFR, phospho-AKT (Ser473), AKT, phospho-Erk1/2 (Thr202/Tyr204), Erk1/2, caspase-3, PARP, GAPDH, β-Tubulin (Cell Signaling Technology, Danvers, MA, USA); HER2 (Santa Cruz Biotechnology, Santa Cruz, CA, USA), and Actin (Sigma-Aldrich, St Louis, MO, USA)]. Then, the cells were incubated with horseradish peroxidase-conjugated secondary anti-rabbit or anti-mouse IgG (Jackson ImmunoResearch Laboratories Inc, West Grove, PA, USA). The immunoreactive proteins were detected using an enhanced chemiluminescence detection reagent (Thermo Fisher Scientific, Rockford, IL, USA). Images were captured with an ImageQuant LAS 4000 biomolecular imager (GE Healthcare, Chalfont St Giles, UK).

Wound-healing assay

For wound-healing experiments, HUVECs (2×10^4) were seeded into 96-well plates in complete medium until a confluent monolayer was formed. The cell monolayer was scratched with a 96-pin WoundMaker (Essen Bioscience, Michigan, USA) and then washed twice with PBS to remove debris, which was followed by the addition of fresh medium that contained various concentrations of DCLAK11. Wound images were

automatically acquired and registered by Incucyte™ (ESSEN BioScience Inc, Ann Arbor, Michigan, USA) every 2 h using the ''scratch wound'' scan type selection. The data were then analyzed using an integrated metric: area under the curves.

Endothelial cell migration assay

A Transwell migration assay was performed in a 24-well chamber (Costar 3422, Corning Life Science, Tewksbury, MA, USA). Cells (4×10^4) were resuspended in serum-free medium in the upper chamber, while the bottom chambers were filled with medium supplemented with 20% FBS. Various concentrations of DCLAK11 were added to both chambers. The cultures were maintained for 8 h, and then the migrating cells were fixed in 90% chilled ethyl alcohol for 30 min at 4 °C and stained with 0.1% crystal violet for 15 min at room temperature. The upper membrane of the insert was swabbed to remove the cells that had not migrated. All images were obtained with a microscope (Olympus Optical Co, Ltd, Tokyo, Japan). The dye that was taken up by the cells was bound to the membrane and was released by the addition of 100 μL of 10% acetic acid; then, the absorbance of the resulting solution was measured at 600 nm with a SpectraMax 190 Microplate Reader (Molecular Devices, USA). Finally, the inhibition rate was calculated as a percentage relative to the control.

Tube formation assay

For the tube formation assay, chilled Matrigel (BD Bioscience, San Jose, CA, USA, 354234) (60 μL/well, no dilution) was added to a chilled 96-well plate on ice and allowed to polymerize for 30 min at 37 °C. The HUVECs (1.5×10^4) were seeded onto each well of the Matrigel-coated 96-well plate and then incubated in medium or with various concentrations of DCLAK11 at 37 °C, whereas medium alone was used as the basal control. After 8 h of incubation, the number of formed networks was determined. Quantitation was performed by counts of the number of tubules with branch points at both ends, and the inhibition rate was calculated as a percentage relative to the control.

Aortic ring assay

The aortas isolated from 6-wk-old male Sprague-Dawley rats were cleaned of periadventitial fat and connective tissues and were cut into 1-mm-long rings. After they were rinsed in PBS, the aortic rings were placed into the 96-well culture plates and sealed in place with an overlay of 50 μL of chilled Matrigel (no dilution). The Matrigel was polymerized for 30 min at 37 °C. The artery rings were cultured in a final volume of 100 μL of serum-free M199 medium with or without various concentrations of DCLAK11. After 7 d, the microvessel growth was measured after images were obtained with a microscope (Olympus Optical Co, Ltd, Tokyo, Japan). The area of the capillary was measured using Adobe Photoshop software (DMC advanced program). Each value represents the average of 3 culture samples. The area of the microvessels was measured using Image-Pro Plus 6.0 software (Media Cybernetics, Bethesda, MD, USA), and the inhibition rate was calculated as a percentage relative to the control.

Statistical analysis

The results are expressed as the mean±SD. The statistical significance was determined using a one-way analysis of variance (ANOVA) and Student's *t*-test for paired data. A P-value<0.05 was considered statistically significant. The calculations were performed with SPSS (Statistical Package for the Social Sciences) for Windows Version 13.0 software (SPSS, Chicago, IL, USA). Mapping was performed with GraphPad Prism 5 (GraphPad Software, San Diego, CA, USA).

Results

DCLAK11 inhibits the activities of multiple tyrosine kinases

We first examined the inhibitory activities of DCLAK11 against a panel of tyrosine kinases, which according to ELISA, are verified targets in cancer therapy. As shown in Table 1, DCLAK11 potently inhibited the activities of the EGFR, HER2, and VEGFR2 tyrosine kinases (IC_{50}<50 nmol/L). In addition, DCLAK11 exhibited a moderate impact on EPH-A2, Flt-1, PDGFR-α, and FGFR1 with IC_{50} values in the range of 50 to 200 nmol/L. In contrast, DCLAK11 only exhibited marginal inhibition of IGF1R (IC_{50}≈1000 nmol/L), c-Met, c-Kit, and FLt-3 (IC_{50}>1000 nmol/L). These data suggested that DCLAK11 is a multi-kinase inhibitor that primarily targets EGFR, HER2, and VEGFR2.

Table 1. Effects of DCLAK11 on the activity of a panel of tyrosine kinases. Kinase activity was assayed by ELISA. IC_{50} values are shown as Mean±SD. n=3.

Kinase	IC_{50} (nmol/L)±SD
EGFR	6.5±0.2
ErbB2	18.0±1.0
VEGFR2	31.3±1.6
EPH-A2	62.6±3.2
Flt-1	80.0±1.0
PDGFR-α	126.0±6.0
FGFR1	185.3±2.2
IGF1R	998.0±81.0
c-Met	>1000
c-Kit	>1000
FLt-3	>1000

EGFR, epidermal growth factor receptor; VEGFR2, vascular endothelial growth factor receptor 2; EPH-A2, ephrin type-A receptor 2; Flt, Fms-like tyrosine kinase; PDGFR-α, platelet derived growth factor receptor-α; FGFR1, fibroblast growth factor receptor1; IGF1R, Insulin-like growth factor 1R.

DCLAK11 inhibits the proliferation of cancer cells

The anti-proliferative activity of DCLAK11 was assessed using a broad panel of human cancer cell lines derived from different types of cancer as well as normal human cells (Table 2). In particular, HCC827 and PC9 cells with EGFR exon 19 dele-

Table 2. DCLAK11 inhibits the proliferation of cancer cells. The anti-proliferation activity of DCLAK11 against a panel of human cancer cell lines and normal human cells originating from different tissue types was determined by SRB or CCK8 assay. The IC_{50} values were plotted as the mean±SD (μmol/L) from three separate experiments.

Cell lines	IC_{50} (μmol/L)±SD
N87	0.02±0.00
BT474	0.08±0.00
HCC827	0.01±0.00
PC9	0.02±0.01
HCC4006	0.02±0.00
A-431	0.40±0.04
H1975	1.27±0.11
MKN45	0.34±0.01
SNU5	0.46±0.07
MCF7	0.39±0.04
MKN-1	0.42±0.08
HL-60	0.70±0.25
MKN74	1.36±0.21
MDA-MB-435	1.43±0.25
SMMC-7721	1.47±0.21
BEL-7402	1.30±0.23
DU145	2.56±0.66
GES-1	0.64±0.01
LO2	1.05±0.07

tions (E746-A750 deletion), HCC4006 cells with both EGFR exon 19 deletions and mutations (L747-E749 deletion, A750P), as well as NCI-N87, BT-474 cells with HER2 gene amplification were included to examine the impact of DCLAK11 on EGFR- or HER2-driven cancer cell growth. As shown in Table 2, DCLAK11 exhibited broad anti-cancer effects but with great variations in potency. The most remarkable activity was observed in the EGFR-aberrant HCC827, PC9, and HCC4006 cell lines, with IC_{50} values of 12, 16, and 22 nmol/L, respectively, and in HER2-amplified NCI-N87 (IC_{50}=19 nmol/L) and BT474 cells (IC_{50}=81 nmol/L). In contrast, DCLAK11 showed 4- to 31-fold less potency in the other cancer cell lines that are known to lack either EGFR or HER2 alterations.

These data demonstrated the advantage of DCLAK11 in the inhibition of EGFR- or HER2-driven cancer cell proliferation. We next proceeded to assess the impact of DCLAK11 on EGFR and HER2 signaling pathways.

DCLAK11 inhibits EGFR signaling and induces apoptosis in EGFR- addicted cells

We next examined the effect of DCLAK11 on EGFR signaling in HCC827 and HCC4006 cells. As shown in Figure 2A and 2B, EGFR phosphorylation was largely inhibited by DCLAK11 in both HCC827 (Figure 2A) and in HCC4006 (Figure 2B) cells in a time- and concentration-dependent manner. AKT and Erk1/2 are two major signaling molecules that function downstream of activated EGFR to drive diverse cellular events[33]. In addition to EGFR inhibition, we also observed the effective inhibition of both AKT and Erk1/2 phosphorylation, which suggests the complete blockage of the EGFR signaling by DCLAK11.

Apoptosis is one of the major cellular events that may account for the cell death that results from EGFR signaling deprivation. We therefore measured the number of apoptotic cells by Annexin V-PI dual staining in HCC827 and HCC4006 cells after DCLAK11 treatment. Indeed, apoptosis occurred in a concentration-dependent manner following 48 h of DCLAK11 treatment in both HCC827 and HCC4006 cells without the concomitant occurrence of necrosis (Figure 3). For example, the apoptotic rate of HCC827 cells (Figure 3A) increased from 13.56% (untreated group) to 62.87% (30 nmol/L DCLAK11 treated group); the apoptotic rate of HCC4006 cells (Figure 3B) increased from 6.36% (untreated group) to 33.53% (100 nmol/L DCLAK11 treated group). The occurrence of apoptosis was further supported by the cleavage of caspase-3 and poly ADP-ribose Polymerase (PARP) (Figure 3C and 3D). After DCLAK11 treatment, the full-length caspase-3 and PARP proteins were cleaved to generate their active forms in a concentration-dependent manner.

DCLAK11 inhibits HER2 signaling and induces apoptosis in cancer cells with HER2 amplification

Similarly, we also examined the effect of DCLAK11 on HER2 signaling in NCI-N87 and BT474 cells (Figure 4A and 4B). After DCLAK11 treatment, the phosphorylation of HER2 and its key downstream signaling molecules Erk1/2 and AKT were significantly decreased in NCI-N87 (Figure 4A) and BT474 cells (Figure 4B) in a concentration- and time-dependent manner.

Cell apoptosis induced by DCLAK11 was also measured. As shown in Figure 5, DCLAK11 induced apoptosis in a concentration-dependent manner in NCI-N87 and BT474 cells following 48 h treatment without an induction of necrosis. In HER2-amplified NCI-N87 (Figure 5A) and BT474 cells (Figure 5B), the apoptotic rate increased by 3-fold after treatment with 300 nmol/L DCLAK11 compared with the untreated group. In agreement with the increased rate of apoptosis, the cleavage of caspase-3 and PARP was detected after DCLAK11 treatment (Figure 5C and 5D).

DCLAK11 inhibits angiogenesis

Our above results validated the effect of DCLAK11 in the inhibition of EGFR- and HER2-dependent cancer growth. We next verified whether the inhibition of VEGFR2 by DCLAK11 could result in anti-angiogenic activity. As shown in Figure 6A, DCLAK11 at a concentration of 30 nmol/L, was able to induce a blockage of VEGFR2 phosphorylation and downstream Erk1/2 phosphorylation in HUVECs that naturally overexpress VEGFR2.

Because VEGF has been clearly identified as a positive mediator of endothelial cell proliferation and angiogenesis[34], we examined the effects of DCLAK11 on VEGF-driven HUVEC proliferation. As expected, DCLAK11 displayed significant inhibitory activities against VEGF-driven HUVEC prolif-

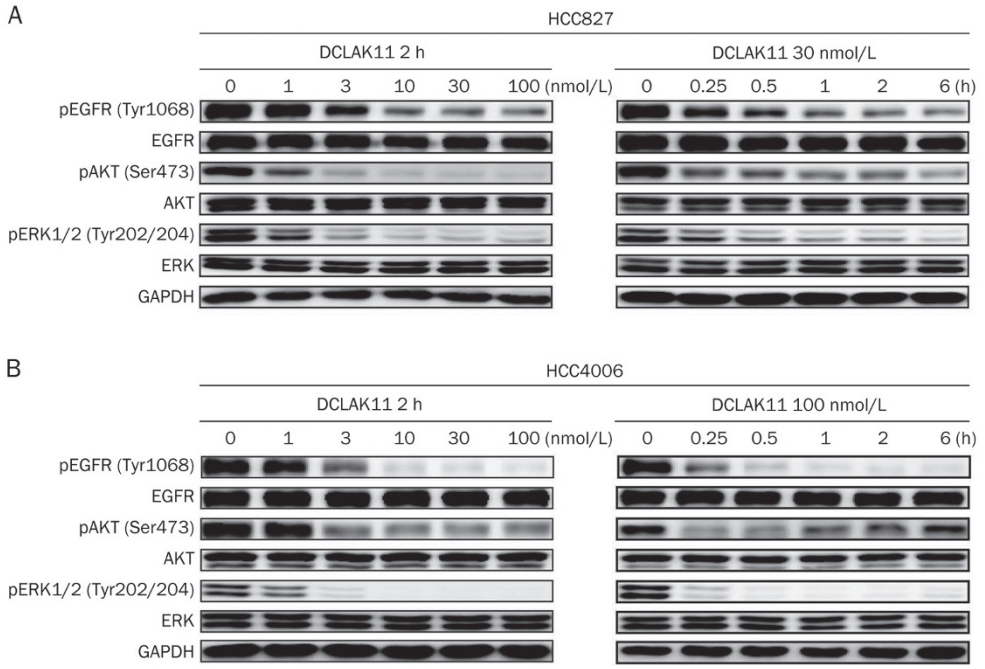

Figure 2. DCLAK11 blocks EGFR phosphorylation and downstream signaling in HCC827 (A) and HCC4006 (B) cells with concentration-dependent and time-dependent manner. Cells were cultured in the presence of different concentrations of DCLAK11 for 2 h or treated with indicated concentrations of DCLAK11 for increasing durations (0.25–6 h), then whole-cell lysates were assayed by Western blots.

eration (IC_{50}=11.07 nmol/L), whereas it demonstrated less potency against FBS-mediated events (IC_{50}=11.08 μmol/L). These results suggested that DCLAK11 impedes VEGF-driven growth of endothelial cells.

Endothelial cell migration is an essential step in angiogenesis, as shown in Figure 6B and 6C, as DCLAK11 suppressed migration of HUVECs in both wound-healing and Transwell assays compared with non-treated cells. As tube formation represents one of the late stages of angiogenesis, we evaluated the effects of DCLAK11 on tube formation in HUVECs on a Matrigel substratum. In the control group, HUVECs formed a mesh of tubes within 8 h, while DCLAK11 reduced the tube formation ability of HUVECs in a concentration-dependent manner with a significant reduction observed at 10 nmol/L (Figure 6D). Almost no tube formation was observed after treatment with DCLAK11 at a concentration of 300 nmol/L.

We further evaluated the anti-angiogenic effects of DCLAK11 in a model of angiogenesis using the rat aortic ring assay. We found that new microvessels grew proficiently when untreated control cultures were incubated for 7 d, while a significant inhibition of microvessel sprouting was observed after treatment with 30 nmol/L DCLAK11 (Figure 6E); again, this effect occurred in a concentration-dependent manner.

Discussion

A functional link between HER family members and VEGF has been established. Accumulating evidence from the literature suggests that a combined blockade of HER- and VEGFR-dependent signal transduction pathways might lead to beneficial clinical effects[35]. This is a tentative inference that multi-tyrosine kinase inhibitor targeting EGFR, HER2, and VEGFR2 may be a viable treatment for cancer.

Through optimization of the hit compound, we obtained DCLAK11, a single compound that inhibits both EGFR/HER2 as well as VEGFR tyrosine kinases.

When profiled as an inhibitor of the HER family and the VEGFR2 of tyrosine kinases, DCLAK11 inhibited both the EGFR/ErbB2 and VEGFR enzymes with low nanomolar IC_{50} values in our ELISA-based kinase inhibitory assays. Furthermore, we observed effects of DCLAK11 on cell signaling and proliferation. DCLAK11 effectively blocked the phosphorylation of EGFR in *EGFR* gene-sensitive mutant cell lines HCC827 and HCC4006, and the phosphorylation of HER2 in cell lines with HER2 gene amplification (NCI-N87 and BT474). Moreover, we found that its activity was modulated by blocking the phosphorylation of AKT and ERK. Together with the potent inhibition of EGFR-mediated proliferation in HCC827 and HCC4006 cells and HER2-mediated proliferation in NCI-N87 and BT-474 cells, compared with other EGFR- or HER2-independent cells, the data strongly suggest that DCLAK11 indeed effectively targets both receptors at the cellular level.

Our data also confirmed the induction of robust concentration-dependent apoptosis by DCLAK11 in both EGFR-mutant and HER2-amplified cell lines. Upon examination of apoptotic pathways, we observed the activation of caspase-3 and PARP, which may have been induced by DCLAK11. This indicates that apoptotic pathways may be involved in DCLAK11-induced cell death. Additionally, DCLAK11 is a potent

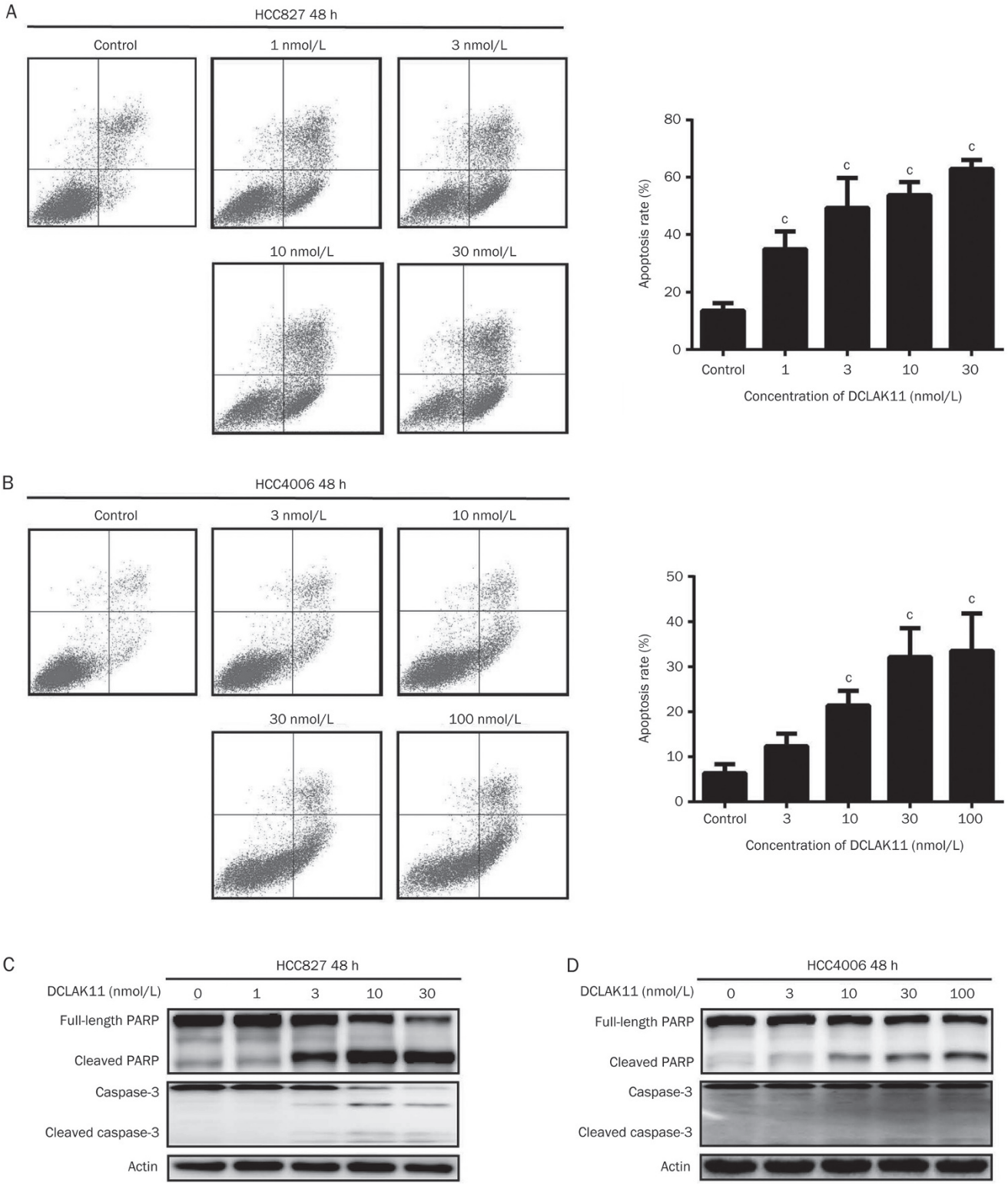

Figure 3. HCC827 (A) and HCC4006 (B) cells were treated with increasing doses of DCLAK11 for 48 h and apoptotic rate was detected by flow cytometry with Annexin V-PI staining. Data are shown as mean±SD from three independent experiments. $^{c}P<0.01$ *vs* control. Western blots were performed to observe the cleaved caspase-3 (Asp175), caspase-3, cleaved PARP and full-length PARP protein expression in HCC827 (C) and HCC4006 (D) cells respectively. The more cleaved caspase-3 and cleaved PARP expression represents for the higher level of apoptosis. Representative data are shown.

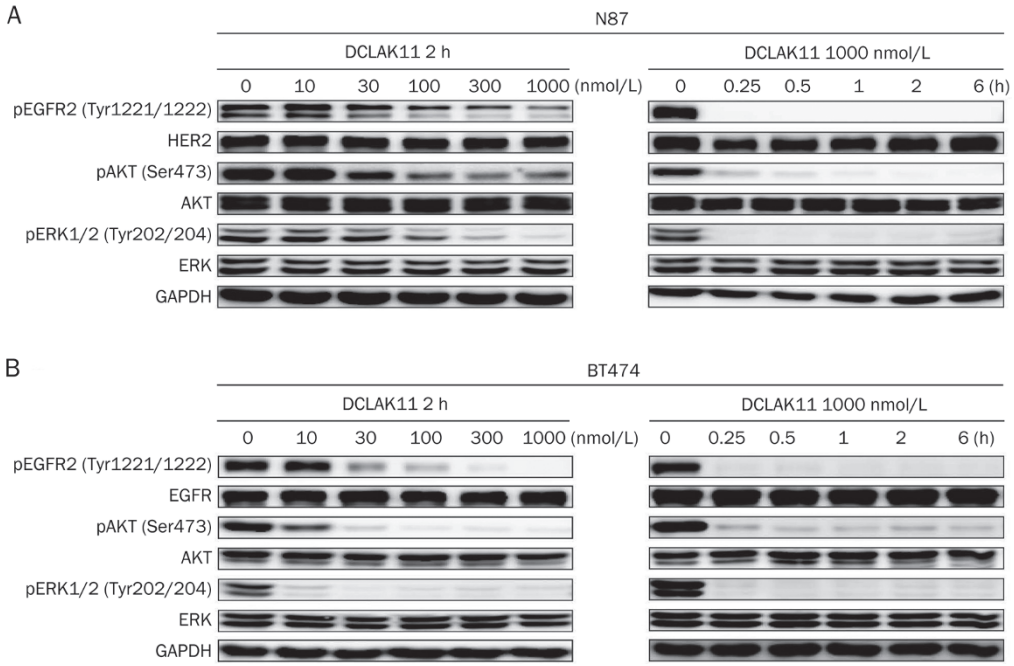

Figure 4. DCLAK11 inhibits HER2 signaling and induces apoptosis in cancer cells with HER2 amplification. (A, B) Concentration- and time-dependent inhibitive activity of DCLAK11 on HER2, AKT, and Erk1/2 phosphorylation in NCI-N87 (A) and BT474 (B) cells. Cells treated with increasing concentrations of DCLAK11 for 2 h or treated with indicated concentrations of DCLAK11 for increasing durations (0.25–6 h) were lysated and subjected to Western blot analysis.

VEGFR2 inhibitor; it inhibited VEGFR2 phosphorylation in HUVECs, which suggests that VEGFR2 signal transduction pathways are affected in this endothelial cell system.

Steps in the growth of new vessels include the migration of endothelial cells from the parent vessel toward the site where angiogenesis is required, the proliferation of endothelial cells behind the front of migration, and the organization of the endothelial cells into capillary-like structures[36]. Therefore, we used a series of assays to recapitulate this multi-step process to evaluate the anti-angiogenic activities of DCLAK11. As expected, DCLAK11 exhibited anti-angiogenic effects, as determined by the inhibition of VEGF-stimulated proliferation, migration and tube formation of HUVECs and on the microvessel growth of rat aortic rings in a concentration-dependent manner. The concomitant anti-angiogenic effects of DCLAK11 should be part of a synergistic outcome of this broad-spectrum inhibitory action.

To conclude, we have shown that DCLAK11 not only inhibits the EGFR/HER2-mediated signal transduction pathway but also blocks VEGFR2-mediated events. We have also demonstrated that the anti-tumor activity of DCLAK11 is accompanied by significant anti-angiogenic activity. In addition, the features of the kinase-inhibitory effects of DCLAK11 on EGFR/HER2 and VEGFR2 provide a scientific basis for the development of multi-targeted anti-cancer drugs.

Acknowledgements

We gratefully acknowledge financial support from the National Natural Science Foundation of China for Innovation Research Group (No 81321092), the National Marine "863" project (No 2013AA092902), and the National Natural Science Foundation of China Grants (91229204).

Author contribution

Jian DING and Hong LIU designed the study; Xiao-bin GUO, Lin-jiang TONG, and Xia PENG performed the research; Wei ZHU and Xian-jie CHEN contributed new reagents or analytic tools; Xiao-bin GUO and Hong-chun LIU analyzed the data; Xiao-bin GUO wrote the paper, and Min HUANG revised the manuscript.

Supplementary information

Supplementary Scheme 1 is available at the Acta Pharmacologica Sinica website.

References

1 Hunter T. Tyrosine phosphorylation: thirty years and counting. Curr Opin Cell Biol 2009; 21: 140–6.
2 Hanahan D, Weinberg RA. The hallmarks of cancer. Cell 2000; 100: 57–70.
3 Luo J, Solimini NL, Elledge SJ. Principles of cancer therapy: oncogene and non-oncogene addiction. Cell 2009; 136: 823–37.
4 Herbst RS, Heymach JV, Lippman SM. Lung cancer. N Engl J Med 2008; 359: 1367–80.
5 Seshacharyulu P, Ponnusamy MP, Haridas D, Jain M, Ganti AK, Batra SK. Targeting the EGFR signaling pathway in cancer therapy. Expert Opin Ther Targets 2012; 16: 15–31.
6 Bose R1, Kavuri SM, Searleman AC, Shen W, Shen D, Koboldt DC, *et al*. Activating HER2 mutations in HER2 gene amplification negative

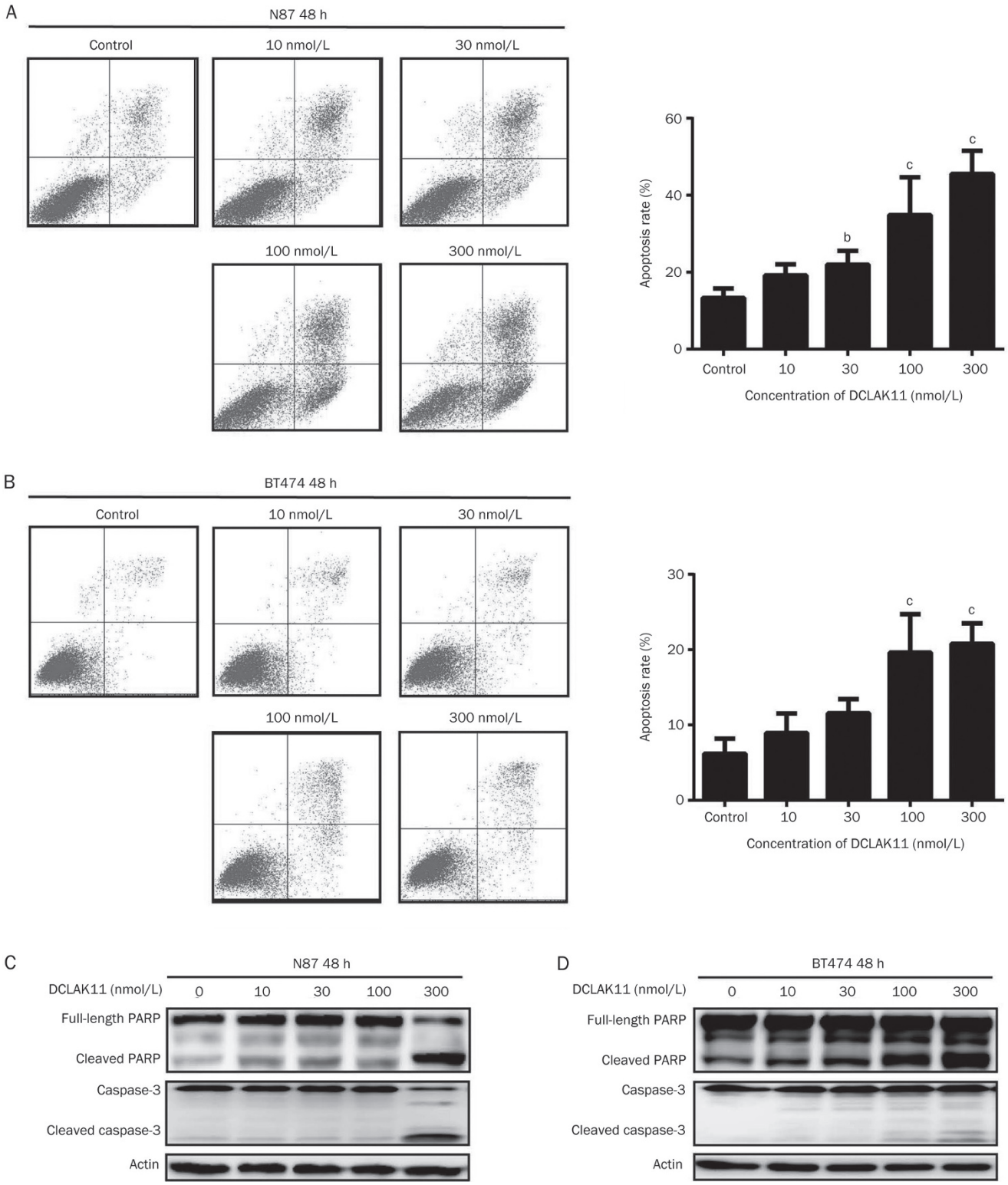

Figure 5. DCLAK11 induces apoptosis in cancer cells with HER2 amplification. (A, B) N87 (A) and BT474 (B) cells were treated with increasing concentrations of DCLAK11 and apoptotic rate was detected by flow cytometry with Annexin V-PI staining. Data are shown as mean±SD from three independent experiments. $^{b}P<0.05$, $^{c}P<0.01$ *vs* control. (C, D) Western blots were performed to observe the cleaved caspase-3 (Asp175), caspase-3, cleaved PARP and full-length PARP protein expression in N87 (C) and BT474 (D) cells, respectively. The more cleaved caspase-3 and cleaved PARP expression represents for the higher level of apoptosis. Representative data are shown.

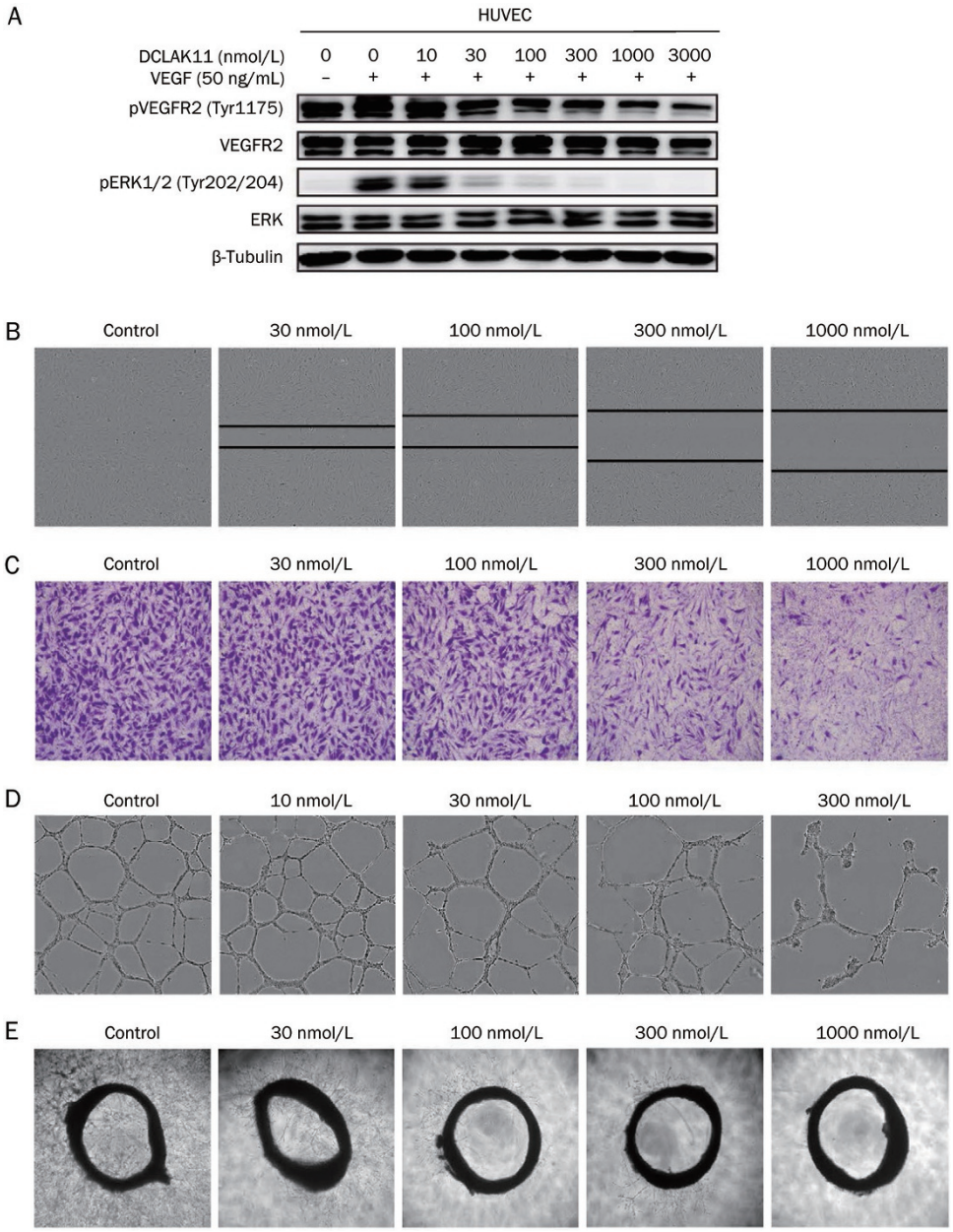

Figure 6. DCLAK11 exhibits antiangiogenic activities. (A) DCLAK11 inhibits the VEGF-stimulated VEGFR2 phosphorylation and signal transduction. HUVECs were starved, then incubated with indicated concentrations of DCLAK11 for 6 h, and VEGF165 (50 ng/mL) was added to the cultures during the last 10 min. Protein samples were subjected to Western blot analysis. Representative data are shown. (B) Effects of DCLAK11 on the migratory ability of HUVECs (wound-healing test). HUVECs were grown to confluence in complete media, wound were made using 96 well WoundMaker and culture in absence or presence of the different concentrations of DCLAK11. (C) DCLAK11 inhibits HUVEC migration in a transwell migration assay. HUVECs treated with various concentrations of DCLAK11 were seeded in both chambers. The upper chamber was filled with serum-free medium, and the bottom chamber was filled with the complete medium containing 20% FBS. (D) DCLAK11 inhibits tube formation of HUVECs. Cells were placed in 96-well plates coated with Matrigel. The tubular structures were photographed after 8 h treatment of DCLAK11. (E) Effect of DCLAK11 on sprouting from rat aortic segments. Rat aortic segments were cultured on Matrigel and treated various concentrations of DCLAK11 for 7 d.

breast cancer. Cancer Discov 2013; 3: 224–37.
7 Lee J, Ou SH. Towards the goal of personalized medicine in gastric cancer--time to move beyond HER2 inhibition. Part I: Targeting receptor tyrosine kinase gene amplification. Discov Med 2013; 15: 333–41.
8 Stephens P1, Hunter C, Bignell G, Edkins S, Davies H, Teague J, *et al*. Lung cancer: intragenic ERBB2 kinase mutations in tumours. Nature 2004; 431: 525–6.
9 Shawver LK, Slamon D, Ullrich A. Smart drugs: tyrosine kinase inhibitors in cancer therapy. Cancer Cell 2002; 1: 117–23.
10 Hubbard SR. Protein tyrosine kinases: autoregulation and small-molecule inhibition. Curr Opin Struct Biol 2002; 12: 735–41.

11 Huang M, Shen A, Ding J, Geng M. Molecularly targeted cancer therapy: some lessons from the past decade. Trends Pharmacol Sci 2014; 35: 41–50.
12 Gschwind A, Fischer OM, Ullrich A. The discovery of receptor tyrosine kinases: targets for cancer therapy. Nat Rev Cancer 2004; 4: 361–70.
13 Baselga J, Albanell J. Epithelial growth factor receptor interacting agents. Hematol Oncol Clin North Am 2002; 16: 1041–63.
14 Grandis JR, Sok JC. Signaling through the epidermal growth factor receptor during the development of malignancy. Pharmacol Ther 2004; 102: 37–46.
15 Tzahar E1, Waterman H, Chen X, Levkowitz G, Karunagaran D, Lavi S, *et al*. A hierarchical network of interreceptor interactions determines signal transduction by Neu differentiation factor/neuregulin and epidermal growth factor. Mol Cell Biol 1996; 16: 5276–87
16 Graus-Porta D, Beerli RR, Daly JM, Hynes NE. ErbB-2, the preferred heterodimerization partner of all ErbB receptors, is a mediator of lateral signaling. EMBO J 1997; 16: 1647–55.
17 Pinkas-Kramarski R1, Soussan L, Waterman H, Levkowitz G, Alroy I, Klapper L, *et al*. Diversification of Neu differentiation factor and epidermal growth factor signaling by combinatorial receptor interactions. EMBO J 1996; 15: 2452–67.
18 Knuefermann C, Lu Y, Liu B, Jin W, Liang K, Wu L, *et al*. HER2/PI-3K/Akt activation leads to a multidrug resistance in human breast adenocarcinoma cells. Oncogene 2003; 22: 3205–12.
19 Folkman J. Tumor angiogenesis: therapeutic implications. N Engl J Med 1971; 285: 1182–6.
20 Folkman J. Endothelial cells and angiogenic growth factors in cancer growth and metastasis. Introduction. Cancer Metastasis Rev 1990; 9: 171–4.
21 Rini BI. Vascular endothelial growth factor-targeted therapy in renal cell carcinoma: current status and future directions. Clin Cancer Res 2007; 13: 1098–106.
22 Ferrara N, Davis-Smyth T. The biology of vascular endothelial growth factor. Endocr Rev 1997; 18: 4–25.
23 Bergers G, Benjamin LE. Tumorigenesis and the angiogenic switch. Nat Rev Cancer 2003; 3: 401–10
24 Rini BI. Vascular endothelial growth factor-targeted therapy in renal cell carcinoma: current status and future directions. Clin Cancer Res 2007; 13: 1098–106.
25 Bhargava P, Robinson MO. Development of second generation VEGFR tyrosine kinase inhibitors: current status. Curr Oncol Rep 2011; 13: 103–11.
26 Viloria-Petit A, Crombet T, Jothy S, Hicklin D, Bohlen P, Schlaeppi JM, *et al*. Acquired resistance to the antitumor effect of the epidermal growth factor receptor-blocking antibodies *in vivo*: a role for altered tumor angiogenesis. Cancer Res 2001; 61: 5090–101.
27 Ferrara N, Kerbel RS. Angiogenesis as a therapeutic target. Nature 2005; 438: 967–74.
28 Ciardiello F, Bianco R, Damiano V, Fontanini G, Caputo R, Pomatico G, *et al*. Antiangiogenic and antitumor activity of anti-epidermal growth factor receptor C225 monoclonal antibody in combination with vascular endothelial growth factor antisense oligonucleotide in human GEO colon cancer cells. Clin Cancer Res 2000; 6: 3739–47.
29 Jung YD, Mansfield PF, Akagi M, Takeda A, Liu W, Bucana CD, *et al*. Effects of combination anti-vascular endothelial growth factor receptor and anti-epidermal growth factor receptor therapies on the growth of gastric cancer in a nude mouse model. Eur J Cancer 2002; 38: 1133–40
30 Yazici S, Kim SJ, Busby JE, He J, Thaker P, Yokoi K, *et al*. Dual inhibition of the epidermal growth factor and vascular endothelial growth factor phosphorylation for antivascular therapy of human prostate cancer in the prostate of nude mice. Prostate 2005; 65: 203–15.
31 Herbst RS, Johnson DH, Mininberg E, Carbone DP, Henderson T, Kim ES, *et al*. Phase I/II trial evaluating the antivascular endothelial growth factor monoclonal antibody bevacizumab in combination with the HER-1/epidermal growth factor receptor tyrosine kinase inhibitor erlotinib for patients with recurrent non-small-cell lung cancer. J Clin Oncol 2005; 23: 2544–55.
32 Guo XN, Zhong L, Zhang XH, Zhao WM, Zhang XW, Lin LP, *et al*. Evaluation of active recombinant catalytic domain of human ErbB-2 tyrosine kinase, and suppression of activity by a naturally derived inhibitor, ZH-4B. Biochim Biophys Acta 2004; 1673: 186–93.
33 Yarden Y, Pines G. The ERBB network: at last, cancer therapy meets systems biology. Nat Rev Cancer 2012;12: 553–63.
34 Ciardiello F, Caputo R, Damiano V, Caputo R, Troiani T, Vitagliano D, *et al*. Antitumor effects of ZD6474, a small molecule vascular endothelial growth factor receptor tyrosine kinase inhibitor, with additional activity against epidermal growth factor receptor tyrosine kinase. Clin Cancer Res 2003; 9: 1546–56.
35 Tortora G, Ciardiello F, Gasparini G. Combined targeting of EGFR dependent and VEGF-dependent pathways: rationale, preclinical studies and clinical applications. Nat Clin Pract Oncol 2008; 5: 521–30.
36 Vailhé B, Vittet D, Feige JJ. *In vitro* models of vasculogenesis and angiogenesis. Lab Investig 2001; 81: 439–52.